

## Article

# Climatological Study of Air Pollutant Emissions in Saudi Arabia

Motirh Al-Mutairi <sup>1</sup>, Nahaa Al-Otaibi <sup>2</sup> , Amgad Saber <sup>3</sup> , Heshmat Abdel Basset <sup>3</sup> and Mostafa Morsy <sup>3,\*</sup> 

<sup>1</sup> Department of Geography, College of Arts, Princess Nourah bint Abdulrahman University, P.O. Box 84428, Riyadh 11671, Saudi Arabia; mkalmutairy@pnu.edu.sa

<sup>2</sup> Department of Biology, College of Science, Princess Nourah bint Abdulrahman University, P.O. Box 84428, Riyadh 11671, Saudi Arabia; namialotaibi@pnu.edu.sa

<sup>3</sup> Department of Astronomy and Meteorology, Faculty of Science, Al-Azhar University, Cairo 11884, Egypt; astmet2011@azhar.edu.eg (A.S.); heshmat@azhar.edu.eg (H.A.B.)

\* Correspondence: mostafa\_morsy@azhar.edu.eg; Tel.: +20-112-593-0086

**Abstract:** This study aims to investigate the spatio-temporal distribution, variation, abrupt change, and long-term trends of major pollutant emissions in the Kingdom of Saudi Arabia (KSA) over the period 1960–2020 using the Monitoring Atmospheric Composition and Climate (MACC)/CityZEN EU projects (MACCity) emissions dataset inventory. These pollutants are carbon monoxide (CO), nitrogen oxides (NO<sub>x</sub>), sulfur dioxide (SO<sub>2</sub>), volatile organic compounds (VOCs), black carbon (BC), and organic carbon (OC). Seven stations were selected (Al-Bahah, Abha, Dahra, Jeddah, Riyadh, Qassim, and Ahsa), which correspond to the highest (hotspot) annual pollutant emissions. The annual cycle analysis of the six pollutant emissions revealed that there are four distinct patterns; the first one has one interannual wave while the other three patterns have two interannual waves. The analysis of the different sectors' contributions to pollutant emissions revealed that the energy, transportation, and industries sectors have the highest percentage contributions. Significant abrupt change points were detected in 1970, 1980, 1990, 2000, 2005, and 2010. The development and growth rates in the KSA starting from the early 1970s are attributed to the oil boom. The great increase in pollutant emissions in the early 1980s followed by that in the 1990s up to 2000 is due to an increase in fossil fuel demand, industries, transportation, and energy consumption.

**Keywords:** pollutant emissions; climate variability; long-term trend; Saudi Arabia; abrupt change; annual cycle patterns; energy consumption



**Citation:** Al-Mutairi, M.; Al-Otaibi, N.; Saber, A.; Abdel Basset, H.; Morsy, M. Climatological Study of Air Pollutant Emissions in Saudi Arabia. *Atmosphere* **2023**, *14*, 729. <https://doi.org/10.3390/atmos14040729>

Academic Editor: Hailin Wang

Received: 13 March 2023

Revised: 11 April 2023

Accepted: 13 April 2023

Published: 18 April 2023



**Copyright:** © 2023 by the authors. Licensee MDPI, Basel, Switzerland. This article is an open access article distributed under the terms and conditions of the Creative Commons Attribution (CC BY) license (<https://creativecommons.org/licenses/by/4.0/>).

## 1. Introduction

Continuous increases in the levels of atmospheric pollutants due to irresponsible human activities lead to significant deterioration in air quality not only in megacities but all over the world, exposing populations to health risks and imposing huge economic and social costs [1–4]. The last few decades have witnessed a rapid expansion of urbanization accompanied by an increasing concentration of harmful pollutants and the degradation of air quality, which has become a major issue for environmental policy at the global and local scales [5]. Unsustainable urban development, industrial and agriculture activities, transportation, and energy demand are the major sources of anthropogenic pollutants and aerosols [4,6]. On the other hand, most studies on climate change have focused on the effects on meteorological variables, while the interconnected nature of air pollution and climate change has been recognized in recent decades, as they affect the ecosystem inextricably [6,7]. The primary emitted anthropogenic gases include carbon dioxide (CO<sub>2</sub>), ozone (O<sub>3</sub>), carbon monoxide (CO), nitrous oxides (NO<sub>x</sub>), methane, and non-methane hydrocarbons (NMHCs), alongside with sulfur dioxide (SO<sub>2</sub>), organic carbon (OC), and black carbon (BC) particles [6, 8–10]. These pollutants cause more than 4 million deaths worldwide each year, including nearly 300,000 children under the age of 15, and more than USD 5 trillion in welfare

losses [11]. The impact on life expectancy of particulate pollution is significant especially in the polluted countries, reaching 1.87, 1.85, 1.56, 1.48, 1.28, and 1.25 years in Bangladesh, Egypt, Pakistan, Saudi Arabia, Nigeria, and China, respectively [12]. Since Saudi Arabia contains vast desert areas, it suffers from high concentrations of particulate matter due to dust storms and construction activities, especially with strong winds that lift sand into the atmosphere and cause heavy aerosol loading [13–16]. Transportation and dense vehicles on Saudi Arabian roads cause the emission of volatile organic compounds and greenhouse gases [17]. According to Lim et al. [18], there is a long-range transport of aerosols resulting from oil burning at the oil deposits located in the northeastern parts of Saudi Arabia to the western parts at Makkah, which in turn affects its air quality. Due to the scarcity of air pollution monitoring, the available studies on air pollutants in Saudi Arabia are mainly limited to major urban areas, such as Riyadh [19,20], Makkah [21,22], Yanbu [23,24], and Jeddah [25,26]. The hourly concentrations of NO<sub>x</sub>, NMHCs, O<sub>3</sub>, SO<sub>2</sub> and particulate matter (PM<sub>2.5</sub> and PM<sub>10</sub>) collected from hourly observations at Yanbu in Saudi Arabia were analyzed by Khalil et al. [24]. Their study showed that ozone concentrations did not vary, and the precursors decreased significantly during the periods of Hajj, Ramadan (Islamic month of fasting), Eids, and weekends. A multi-criteria analysis of climate based on various multi-criteria decision-making techniques and metaheuristics is quite popular nowadays [27–29]. Therefore, it is critical to attain an ambient air quality assessment using effective monitoring such as satellite or reanalysis datasets that adequately covers the interested area. This work aims to use the MACCity emissions dataset inventory to achieve the following objectives: (I) analyze the spatiotemporal distribution of the major pollutant emissions over Saudi Arabia during the period 1960–2020 to identify high-emission sites (hotspots); (II) categorize the annual cycle into various patterns based on the highest and lowest emissions across the different months at the identified hotspots (stations); (III) investigate and analyze the annual variability, abrupt change, and long-term trends of these pollutant emissions at the selected stations during the study period (1960–2020).

## 2. Study Area

The Kingdom of Saudi Arabia (KSA) extends geographically to cover the region between the latitudes from 16 to 33° N and longitudes from 34 to 56° E as shown in Figure 1 inside the bold black solid polygon. The KSA is bordered to the east by the United Arab Emirates (U.A.E.), Qatar, and the Arabian Gulf, to the north by Jordan, Iraq, and Kuwait, to the south by Oman and Yemen, and to the west by the Red Sea. The KSA includes five main regions, namely the North region, the Central region, the Eastern region, the Western region, and the Southern region [30,31], as well as the Rub' Al-Khali (Empty Quarter) that covers the southeastern part (Figure 1) of the country [32,33]. The KSA is an arid and semi-arid country that has a desert climate with limited water resources, low rainfall, and high temperatures, particularly during summer [34–36]. Seven stations were identified to facilitate the analysis of the interesting pollutants across the KSA, where their geographical information is described in Table 1 and shown in Figure 1. These seven stations are distributed as follows: two in the Central Region (Riyadh and Qassim), two in the Eastern Region (Dhahran and Ahsa), two in the Western Region (Al-Baha and Jeddah), and one in the Southern Region (Abha). In both the Rub' Al-Khali (Empty Quarter) and the Northern Region, no stations were identified because most of the pollutants have low emission values.



Figure 1. Topographic map of KSA and the locations of the identified seven stations.

Table 1. Geographical information of the selected seven sites with highest emissions (hotspots).

Region	Station	Latitude (°N)	Longitude (°E)	Elevation (m)
Western	Jeddah	21.71	39.18	18
	Al-Baha	20.29	41.64	1655
Southern	Abha	18.23	42.66	2100
Central	Qassim	26.30	43.76	648
	Riyadh	24.92	46.72	612
Eastern	Ahsa	25.30	49.49	180
	Dhahran	26.26	50.16	22

### 3. Data and Methodology

#### 3.1. Acquired Emissions Data

Monthly gridded emissions inventory data with  $0.5^\circ \times 0.5^\circ$  horizontal resolution for six pollutants during a long-term timeseries from 1960 to 2020 (61 years) over Saudi Arabia were obtained from ECCAD (<https://eccad3.sedoo.fr/metadata/443>, accessed on 1 December 2022). The MACCity emissions inventory dataset is a global anthropogenic emissions inventory for the years 1960 to 2020 and is a part of the MACC and CityZen European project, the ACCMIP and the RCP8.5 emissions datasets, which extend on an annual basis for the period from 1960 to 2020 for anthropogenic emissions and from 1960 to 2008 for biomass burning emissions [37]. ACCMIP (Atmospheric Chemistry and Climate Model Intercomparison Project) MACCity anthropogenic emission is linearly interpolated for each sector and species for each year between ACCMIP and RCP8.5 with base years 1960, 1970, 1980, 1990, 2000, 2005, 2010, and 2020 [38].

The considered pollutants in this study are carbon monoxide (CO), nitrogen oxides (NO<sub>x</sub>), sulfur dioxide (SO<sub>2</sub>), black carbon (BC), organic carbon (OC), and non-methane organic compounds (VOCs = C<sub>3</sub>H<sub>6</sub> + C<sub>2</sub>H<sub>6</sub> + C<sub>3</sub>H<sub>8</sub> + C<sub>2</sub>H<sub>4</sub> + CH<sub>2</sub>O + BIGENE + BIGALK + CH<sub>3</sub>CHO + CH<sub>3</sub>COCH<sub>3</sub> + C<sub>2</sub>H<sub>5</sub>OH + CH<sub>3</sub>OH + TOLUENE + MEK). Emissions data

for the six selected pollutants were obtained as emissions from nine sectors (agriculture, agricultural waste, residential, energy, industries, ships, transportation, solvents, and waste), as well as their summation. These emissions data were extracted at the identified seven KSA stations during the study period (1960–2020) to facilitate long-term statistical analysis. The monthly pollutant emissions data were retrieved in  $\text{kg} \times \text{m}^{-2} \cdot \text{s}^{-1}$  and multiplied by  $2592 \times 109$  ( $60 \text{ s} \times 60 \text{ min} \times 24 \text{ h} \times 30 \text{ days} \times 106$ ) to obtain the total monthly values ( $\text{kg} \cdot \text{m}^{-2} \cdot 10^6$ ) of these pollutants.

### 3.2. Methodology

#### 3.2.1. Homogeneity Test

The Bartlett test for homogeneity of variances was performed in this study to assess the homogeneity of pollutant emissions data when considering the Gaussian (normal) distribution of values. The Bartlett test is an inferential method used to find out the equality of variances between different groups (K) within the time series of the considered variable with equal subperiods, where  $K \geq 2$ . The Bartlett test null hypothesis is that all entire groups (K) have equal variances ( $H_0 : \sigma_1^2 = \sigma_2^2 = \sigma_3^2 = \dots = \sigma_K^2$ ), while the alternate hypothesis is that the variances of at least two groups are not equal ( $H_1 : \sigma_1^2 \neq \sigma_2^2 \neq \sigma_3^2 \neq \dots \neq \sigma_K^2$ ). The sample variance  $\sigma_K^2$  is computed from the formula in Equation (1) [39].

$$\sigma_K^2 = \frac{1}{n} \left( \sum x_i^2 - \frac{1}{n} (\sum x_i)^2 \right) \quad (1)$$

where K is the group number, n is the number of records within the group K,  $\Sigma$  is the summation of emissions over the n within the group K, and  $x_i$  is the temporal emission values.

Now, the variance ratio (VR) between the highest group variance ( $\sigma_{k(\max)}^2$ ) to the lowest group variance ( $\sigma_{k(\min)}^2$ ) is defined as in Equation (2).

$$\text{VR} = \frac{\sigma_{k(\max)}^2}{\sigma_{k(\min)}^2} \quad (2)$$

Finally, to determine whether the pollutant emission values within the K groups are homogeneous (have equal variances;  $H_0$ ) or not ( $H_1$ ) requires comparison of the estimated VR value with the critical value given in the Biometrika Table 31 that obtained from reference [40] at a 0.95 confidence level and  $k - 1$  degree of freedom.

#### 3.2.2. Coefficient of Variation (COV)

The coefficient of variation (COV) for the six pollutant emissions at the identified seven KSA stations was determined as the ratio between the standard deviation (SD) and the climate mean ( $\mu$ ) as in Equation (3).

$$\text{COV} = (\text{SD}/\mu) * 100 \quad (3)$$

The coefficient of variation (COV) is the statistical measure that quantifies the dispersion (deviation) of data values within the time series around its climate mean. Low COV values indicate that the dispersion of the data in the timeseries is low and their distribution is closer to the climate mean, while high COV values indicate that the data have wide dispersion and variance around the climate mean.

#### 3.2.3. Trend Analysis

To assess the monotonic trend and its significance in the annual and seasonal emissions of the six pollutants at the selected seven KSA stations, the non-parametric Mann–Kendall (M-K) rank statistical (tau) test [41–43] is used. M-K tau measures the strength and direction of correlation (degree of agreement) between the rank order of the data points within the

timeseries and the degree to which the trend is monotonous. M-K tau values change within the range from  $-1$  to  $+1$ , where positive tau values indicate an upward (increasing) trend and have a perfect positive monotonic trend at  $+1$ , while negative tau values indicate a downward (decreasing) trend and have a perfect negative monotonic trend at  $-1$ . The sequential steps that were followed in this study to estimate the M-K rank correlation statistical (tau) test were explained in detail by [44].

### 3.2.4. Cumulative Annual Mean

The cumulative annual mean (CAM) method [45] was utilized in this study to assess the annual and inter-decadal fluctuations in the pollutant emissions behavior and detect the pollutant emission time-varying structures throughout the study period. CAM is the average of all prior values at each data point in the time series, starting with the first value, followed by computing the next CAM for the first two values, then for the first three values, and continuing until the last time step in which the CAM value is equal to the climate annual average.

The CAM calculation as a function in time can be defined as in Equation (4).

$$\text{CAM}_t = \frac{1}{t} \sum_{j=1}^t x_j, \quad t = 1, 2, \dots, M \quad (4)$$

where  $x_j$  is the annual emission values of the pollutants and  $M$  is the total number of years.

### 3.2.5. Abrupt Change

The significant variations, sudden (abrupt) changes, and the single shift points within the pollutant emissions along the study period at the identified seven KSA stations were investigated using the Mann–Whitney Z (MWZ) statistics of two sample rank-based tests for the step trend [46]. Suppose the pollutant emissions data within the time series are  $X = (x_1, x_2, x_3, \dots, x_t)$ , then the abrupt change detection method will look for the time ( $t$ ) when  $F1 \neq F2$ , where  $F1$  and  $F2$  are different distribution functions for  $Y_1 = (x_1, x_2, \dots, x_n)$  and  $Y_2 = (x_{n+1}, x_{n+2}, \dots, x_m)$ , respectively. The null hypothesis is  $H_0 : F1 = F2$ , which implies that the  $X$  data vector does not have change points over time, while the alternative hypothesis  $H_1 : F1 \neq F2$  indicates that there is an abrupt change point in the distribution of  $X$  at time  $t$ . The MWZ statistics test is of the form shown in Equation (5).

$$\text{MWZ} = \left[ \left( \sum_{t=1}^m U_t \right) - \left( \frac{n(n+m+1)}{2} \right) \right] / \left[ \sqrt{(n * m(n+m+1))/12} \right] \quad (5)$$

where  $U_t$  is the rank of the data points in the complete timeseries of  $n$  sample. The null hypothesis  $H_0 : F1 = F2$  is accepted when  $-Z_{1-ff/2} \leq \text{MWZ} \leq +Z_{1-ff/2}$  and vice versa, where  $ff$  represents significance level of the MWZ statistics test.

## 4. Results and Discussion

### 4.1. Emissions Data Homogeneity

According to the terms of Bartlett's homogeneity test that was applied in this study, the timeseries of pollutant emissions data over the period 1960–2020 (61 years) was divided into six groups ( $K = 6$ ), and each group has 10 years ( $n = 10$ ). The variance ratio (VR) between the maximum and minimum variance ( $\sigma_{k(\max)}^2 / \sigma_{k(\min)}^2$ ) for these six groups at the selected seven KSA stations is shown in Table 2. This estimated VR is compared to the value provided in Biometrika Table 31 [40] at the 95% significance point to determine the critical value for homogeneity of these emissions data, which is 7.80 at  $k = 6$  and  $n = 10$ . If the VR value is greater than the tabulated critical value, this means that the pollutant emissions data are heterogeneous ( $H_1$ ), while they become homogeneous ( $H_0$ ) if the VR value is closer to 1 or less than the tabulated critical value. Therefore, it is noticed that all pollutant emissions data during the study period (1960–2020) at the identified seven KSA

stations are homogeneous, and they can be precisely used for further statistical analysis to assess the natural climate variability and trends.

**Table 2.** Bartlett homogeneity test results for the annual pollutant emissions at the seven stations.

Station	Variance Ratio (VR) = $\sigma_{k(\max)}^2 / \sigma_{k(\min)}^2$					
	CO	NO <sub>x</sub>	SO <sub>2</sub>	VOCs	BC	OC
Jeddah	6.5	4.1	1.6	1.5	7.1	4.8
Al-Baha	7.2	6.9	3.4	2.4	1.3	3.8
Abha	7.5	7.7	1.2	2.3	5.9	4.7
Qassim	6.2	7.6	1.5	0.8	5.2	7.5
Riyadh	7.6	5.4	1.9	0.3	7.1	4
Ahsa	3.2	5.5	2.2	0.8	6	3.8
Dhahran	7.7	3	2.6	2.2	0.7	3.7

#### 4.2. Pollutant Emissions Analysis

In this section, the mapping analysis of the annual average of the monthly emissions of carbon monoxide (CO), nitrogen oxides (NO<sub>x</sub>), sulfur dioxide (SO<sub>2</sub>), volatile organic compounds (VOCs), black carbon (BC), and organic carbon (OC) during the study period (1960–2020) is discussed. In addition, the highest annual pollutant emissions sites (hotspots) are identified, and the maximum and minimum monthly values throughout the study period (1960–2020) are analyzed at these identified sites. Additionally, the behavior of the climatological monthly (annual cycle) emissions at these hotspots over the period of study is investigated to determine the different emissions patterns.

##### 4.2.1. The Spatial Distribution of Pollutant Emissions and Hotspots

The spatial distributions for the annual emissions of the six pollutants are shown in Figure 2. It is noticed that the northern region, the southern part of the eastern region, and the eastern part of the southern region have the minimum pollutant emissions. In addition, the maximum pollutant emissions, associated with large areas of human activity, are detected in the central region, western region, northern part of the eastern region and the western part of the southern region. Additionally, the highest emissions (hotspots) are found in areas with the highest human activities such as big cities, power plants, seaports, oil and gas production, and higher-population-density zones. These hotspots can be clearly identified at seven major locations represented by two stations within the western region (Jeddah and Al-Baha), two stations within the central region (Riyadh and Qassim), two stations within the northern part of the eastern region (Dhahran and Ahsa) and one station within the western part of the southern region (Abha). The geographical information of the identified seven stations (hotspots) is described in Table 1.

The mean annual emissions of the concerned six pollutants at the chosen seven stations during the study period (1960–2020) is shown in Figure 3, where the unit of all values is  $\text{kg} \cdot \text{m}^{-2} \times 10^6$ . It was found that the highest mean annual CO emissions was detected at Dhahran (2462) followed by Riyadh (1165.6) and Ahsa (1060.7). Additionally, the Ahsa, Riyadh, and Dhahran stations have the highest mean annual NO<sub>x</sub> emissions, with values of 781, 580.8, and 414.8, respectively. The Abha, Ahsa, and Riyadh stations have the highest mean annual SO<sub>2</sub> emissions, with values of 2217.2, 1474.2, and 1358.7, respectively. VOCs have the highest mean annual emissions at Dhahran (1970.5), followed by Abha (721) and Al-Baha (485.6), while the highest mean annual BC emissions were detected at Riyadh (41.1), followed by Jeddah (25.6) and Qassim (9.3). The highest mean annual OC emissions were also found at Riyadh (69.9), followed by Dhahran (58.2) and Jeddah (44.1). Additionally, the Al-Baha station has the lowest mean annual emissions for all pollutants except for VOCs at the Qassim station. The pollutants BC and OC had the lowest mean annual emissions compared to the other pollutants.

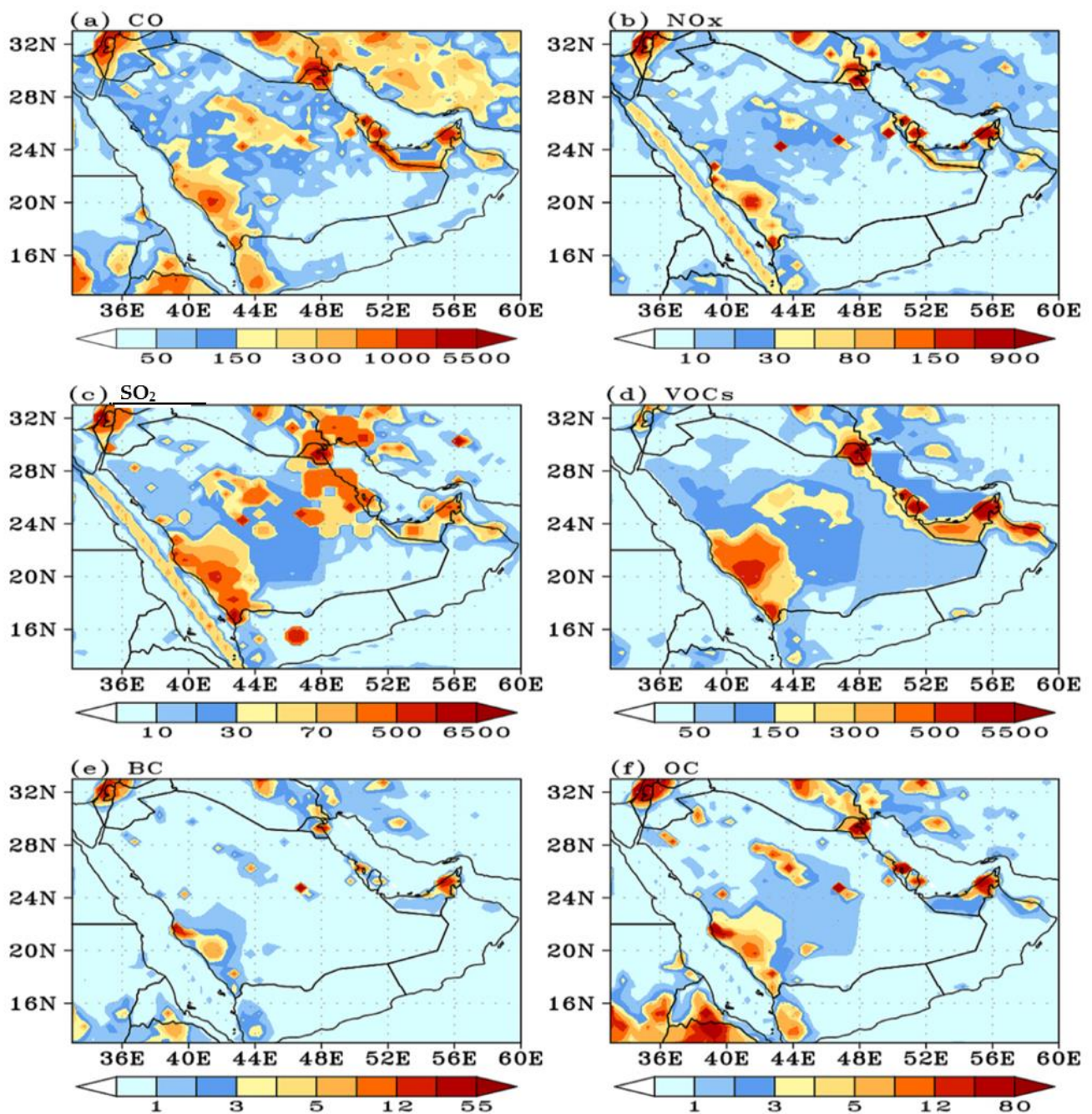


**Figure 2.** The annual pollutant emissions ( $\text{kg}\cdot\text{m}^{-2} \times 10^6$ ) during the period 1960–2020 over KSA.

Table 3 summarizes the maximum and minimum annual emissions of the six pollutants at the seven KSA stations during the study period. The higher maximum annual emissions of CO occur at Dahran, Riyadh and Ahsha while the lowest ones appear at Jeddah (994.3). The highest minimum annual emissions of CO occur at Riyadh, Dahran and Abha while the lowest ones appear at AL-Bahah (30.3). The highest maximum annual emissions of NO<sub>x</sub> occur at Ahsha, Riyadh, and Dahran while the lowest ones appear at Qassim (142.9). The lowest minimum annual emissions of CO occur at Al-Bahah, Jeddah, and Qassim while the highest ones appear at Riyadh (88.2). For SO<sub>2</sub>, there are three stations that have highest values (Abha, Ahsha, Riyadh) followed by Jeddah (1525.9) and Qassim (1169.2), while the lowest maximum annual emissions value of SO<sub>2</sub> (324) appears at Al-Bahah. The minimum annual emissions values of SO<sub>2</sub> are very small compared to their corresponding maximum values. The highest two maximum values of VOCs detected at Dahran and Abha

are followed by those at Al-Baha (934.6), while the lowest two minimum values of VOCs appear at Qassim (78.7) and Al-Bahah (84.8). Table 3 also shows that BC and OC have the lowest maximum and minimum annual emissions compared to the other pollutants.

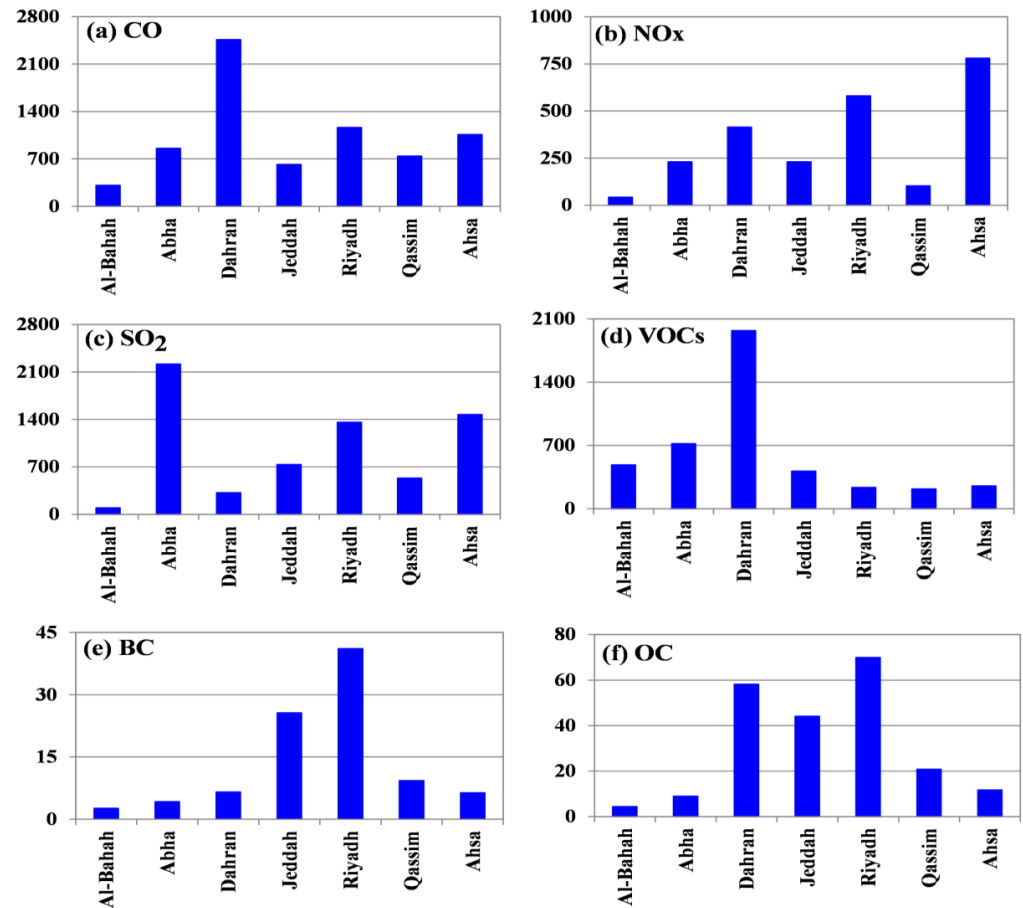


Figure 3. Mean annual pollutant emissions ( $\text{kg}\cdot\text{m}^{-2} \times 10^6$ ) at the seven KSA stations during the study period.

Table 3. The maximum and minimum annual values of all pollutant emissions ( $\text{kg}\cdot\text{m}^{-2} \times 10^6$ ) at the seven KSA stations throughout the study period.

Pollutant		Jeddah	Al-Baha	Abha	Qassim	Riyadh	Ahsa	Dhahran
CO	Max.	994.3	1372.1	1200.2	1050.2	1877.1	1805.5	4052.2
	Min.	281.8	30.3	324.6	255.1	446.0	145.0	391.3
NOx	Max.	363.5	183.5	323.5	142.9	941.7	1308.4	634.0
	Min.	45.1	2.2	65.4	25.6	88.2	75.4	61.3
SO <sub>2</sub>	Max.	1525.9	324.1	4857.8	1169.2	2719.9	2786.8	626.7
	Min.	10.2	1.1	30.3	8.5	18.5	23.8	17.5
VOCs	Max.	576.9	934.6	1043.6	301.3	295.0	361.2	2854.6
	Min.	191.9	84.8	153.7	78.7	138.3	119.2	444.7
BC	Max.	79.9	10.1	7.0	24.5	133.6	19.8	9.2
	Min.	1.8	0.0	0.2	1.3	1.3	0.6	0.7
OC	Max.	142.1	11.8	16.8	50.4	237.8	36.3	83.2
	Min.	6.4	0.0	0.9	6.7	2.9	2.5	32.0

#### 4.2.2. Contribution of Different Sectors to Total Pollutant Emissions

The MACCity anthropogenic emissions inventory for the different nine sectors is used to illustrate the percentage contribution of each sector (%) to the total emission of the selected six pollutants over the seven KSA stations. Figure 4 shows the percentage contribution of each sector (source) to the total emissions of each pollutant at the seven stations. For CO (Figure 4a), it is obvious that the largest contribution comes from transportation (35%), followed by energy (28%) and residential (26%). It is also clear that the participation rate from the agricultural waste sector was small at most stations (6%), while there is not any contribution to CO from the agriculture, ships, and solvents sectors. Figure 4b shows the percentage contribution of each sector (source) for the average total emission of NOx at the seven stations; we find that the highest participation rate (percentage contribution) comes from the energy (42%), transportation (24%), and industries (23%) sectors. The participation rates (percentage contribution) from the other sectors were very small except for residential (9%). Figure 4c illustrates that the industries sector (56%) and energy (34%) represent the largest participation rates in SO<sub>2</sub> emission, while the other seven sectors had very small participation rates, the highest of them being the transportation sector (8%). Figure 4d shows that VOCs are emitted at the highest rate from the energy sector (71%), followed by transportation (15%), then ships (8%), while the other sectors participated at a very small percentage (6%). Figure 4e,f show that the transportation sector has the highest emission rates in both BC and OC, reaching 54% and 56%, respectively, followed by the industries sector in BC with 33% and the energy sector in OC with 24%. While the agricultural waste sector contributes with 9% and 13% to the emissions of BC and OC, respectively, the participation rates of the other sectors were very low.

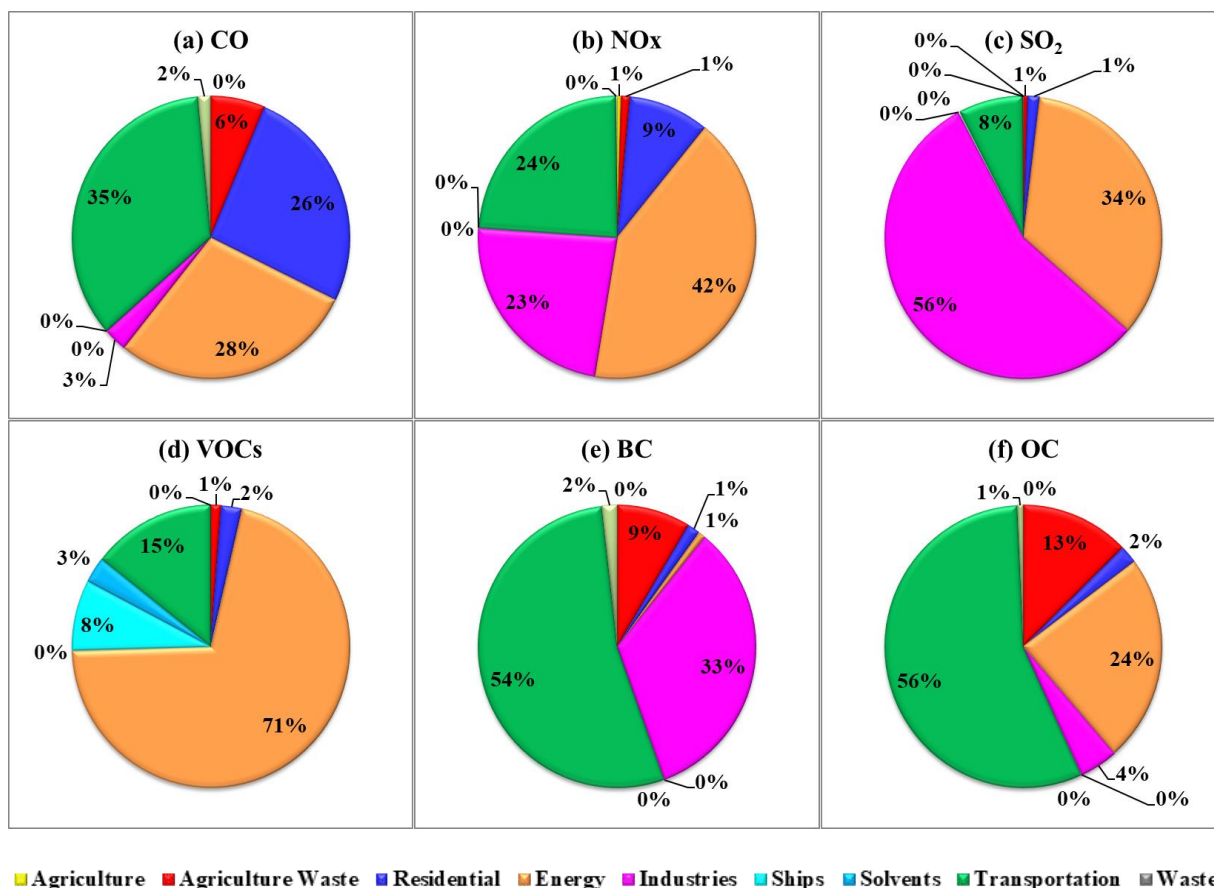
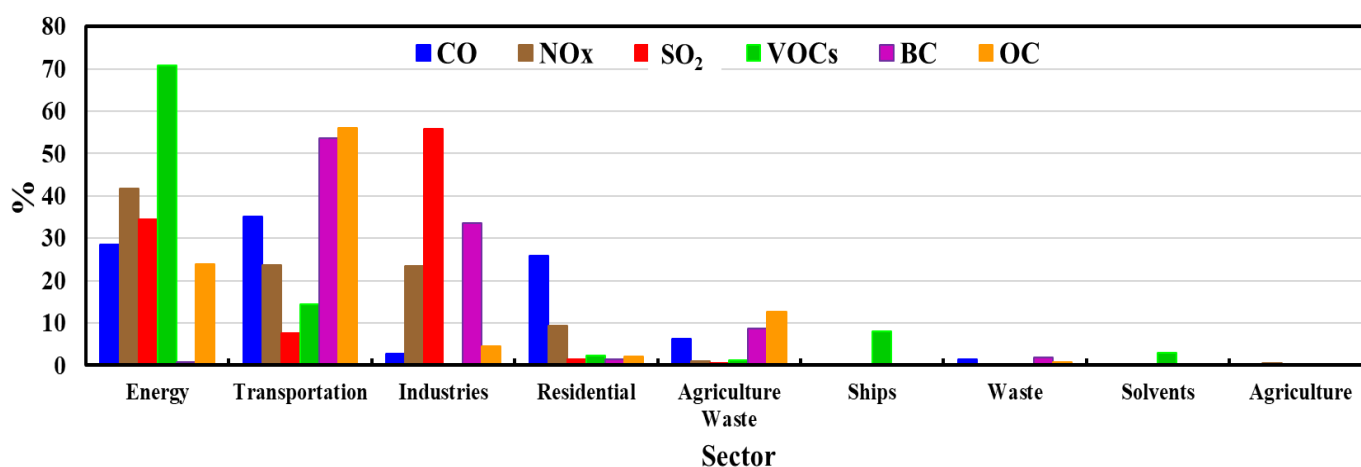


Figure 4. Contribution of the different sectors (%) to the total emission of the selected six pollutants as an average over the seven KSA stations.

Figure 5 summarizes the percentage contribution of each sector to the emission of the six pollutants. The energy sector has the highest percentage contribution to the emission of the six pollutants with the highest one in VOCs (71%) and lowest contribution in BC (1%). Figure 5 also shows that the second sector in the percentage participation is the transportation sector, where it participates at 56% and 54% in the emissions of OC and BC, respectively; the lowest-percentage contribution of transportation is in SO<sub>2</sub> (8%). The industries sector has varying participation rates in all pollutants, where its highest contribution is in SO<sub>2</sub> (56%) while the lowest is in VOCs (0.1%). The contributions of the residential sector were low in most pollutants; the highest-percentage contribution occurs in CO (26%) followed by NO<sub>x</sub> (9%), and the rate of participation for the other pollutants is very small. The agricultural waste, ships, waste, solvents, and agriculture sectors had the lowest participation rates compared to other sectors. The highest participation of the agriculture waste sector is in OC (13%), while the highest participation of the ships sector is in VOCs (8%). The only contribution of the solvents sector appears in VOCs, with 3%. The only contribution of the solvents sector appears in VOCs, with 3%.



**Figure 5.** Contribution of each sector (%) to the six pollutant emissions as an average over the seven stations.

#### 4.2.3. The Behavior of Annual Pollutant Emissions

In this section, we will illustrate the temporal change in the annual values of pollutant emissions at the relevant seven stations, and to do so, we selected three stations for each pollutant to represent the behavior of the annual values across all KSA stations as shown in Figure 6. Generally, there is a slight increase in the emissions of most pollutants at most stations during the 1960s, followed by a moderate increase during the 1970s and a high increase during the 1980s. In addition, the pollutant emissions see the highest increase after 1990, continued up to of the beginning of the 2000s, after which it remains at the same level up to the end of the study period (2020). On the other hand, BC and OC at most stations along with VOCs at the Riyadh station have different behaviors. Where VOCs emissions at the Riyadh station increased during the 1960s and the period 1980–2020, they decreased during the 1970s. Both BC and OC, at the Jeddah, Riyadh, Qassim, and Ahsa stations, have a slight increase in the 1960s and a sharp increase in the 1970s and 1980s, followed by a sharp decrease during the 1990s, followed by reaching the lowest levels during 2000–2020. At the Abha and Dhahran stations, BC and OC follow the same behavior as other pollutants, but at the Al-Baha station, they did not record any emissions during the period 1960–1990, while emissions increased significantly after 1990 up to 2020.

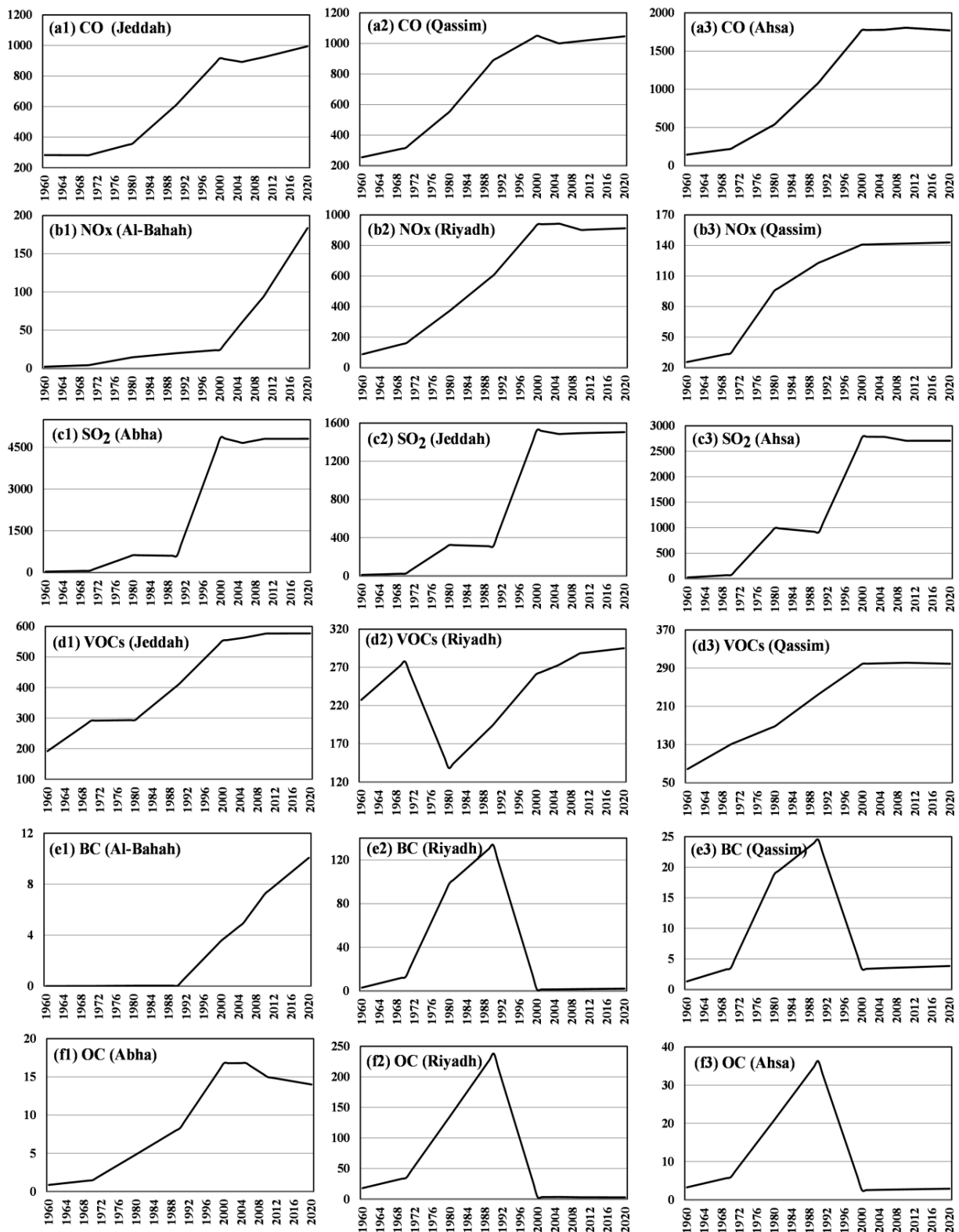


**Figure 6.** Annual emissions ( $\text{kg}\cdot\text{m}^{-2} \times 10^6$ ) at three stations for all pollutants during the study period.

Figure 6 also reveals that the lowest emissions for all pollutants occurred in 1960 at most stations, except at Jeddah for both CO in 1970 and OC in 2020, at Riyadh for both BC in 2000 and VOCs in 1980, and at Ahsa for OC in 2000. During 2020, the highest emissions were recorded at the Al-Baha station for all pollutants (except in 2010 for OC), at Abha

for BC and NO<sub>x</sub>, at Jeddah for CO and VOCs, at Riyadh for CO and VOCs, at Qassim for NO<sub>x</sub>, and at Ahsa for VOCs. Additionally, the highest emissions for both BC and OC are recorded at Jeddah, Riyadh, Qassim, and Ahsa during 1990. During 2000, the detected highest emissions are found at Abha for both CO and SO<sub>2</sub>; at Dhahran for CO, OC, and SO<sub>2</sub>, at Jeddah, Riyadh, and Ahsa for SO<sub>2</sub>; and at Qassim for SO<sub>2</sub>. During 2005, the noted highest emissions are found for OC at Abha and for NO<sub>x</sub> at Dhahran, Jeddah, Riyadh, and Ahsa, while in 2010, they are found for OC at Al-Baha; for VOCs at Abha, Dhahran, and Qassim; for BC at Dhahran; and for CO at Ahsa. Generally, the highest and lowest annual maximum emissions across all pollutants were detected at the Abha station for SO<sub>2</sub> and BC, respectively, while the highest and lowest annual minimum emissions were noticed for CO and BC at the Riyadh and Al-Baha stations, respectively.

#### 4.2.4. Annual Cycle Patterns of Pollutant Emissions

To explain the six pollutant emissions at the seven stations, 42 display panels were required. To overcome the large number of panels and facilitate the pollutants analysis and discussion, the similarity between the emissions behavior of all the pollutants at the seven stations was investigated to identify one pattern for the similar behaviors. Therefore, the behaviors of the climatological monthly emission values of the six pollutants at the selected seven stations during the study period (1960–2020) follow four distinct patterns as shown in Figure 7 and presented separately in Figure 8. The emissions that follow the pattern 1 have one interannual wave with the maximum emissions (peak of the wave) in winter (December, January, and February) and the minimum emissions (bottom of the wave) in summer (June, July, and August) as shown in Figure 7a. Pattern 2 includes the emissions that have two interannual waves, with two maximum emissions in February–April and September, and two minimum emissions in May–August and October–January as shown in Figure 7b. The behavior of the emissions that follow pattern 3 have two interannual waves, with two maximum emissions in the period from mid-winter to mid-spring and in autumn (November), and two minimum in August and December as shown in Figure 7c. The pattern 4 also comprises the emissions that have two interannual waves, with two maximum peaks in March–June and autumn (September–November), and two minimum bottoms in July–August and winter (December–February) as shown in Figure 7d. Thus, pattern 1 contains the emissions that have one wave, while the other three patterns contain the emissions that have two waves, with various highest and lowest values across the different months.

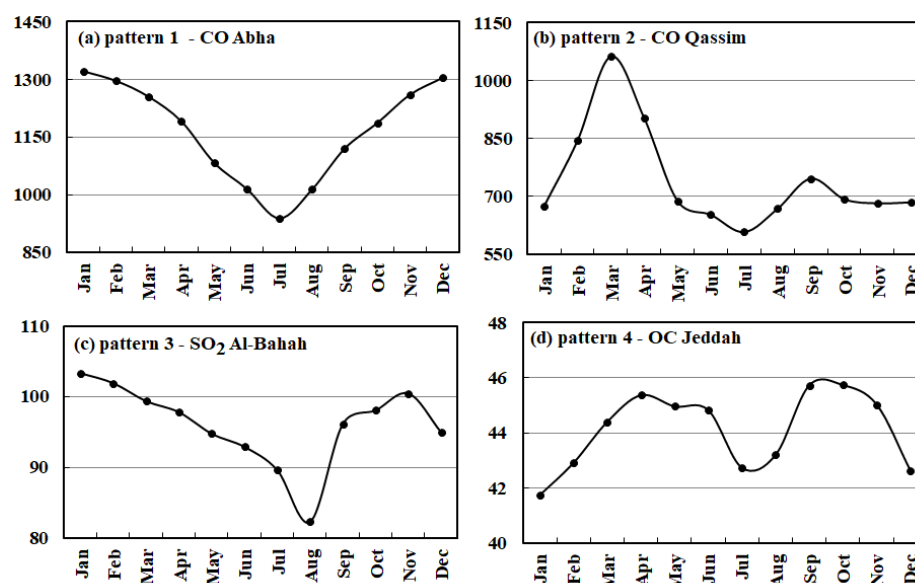
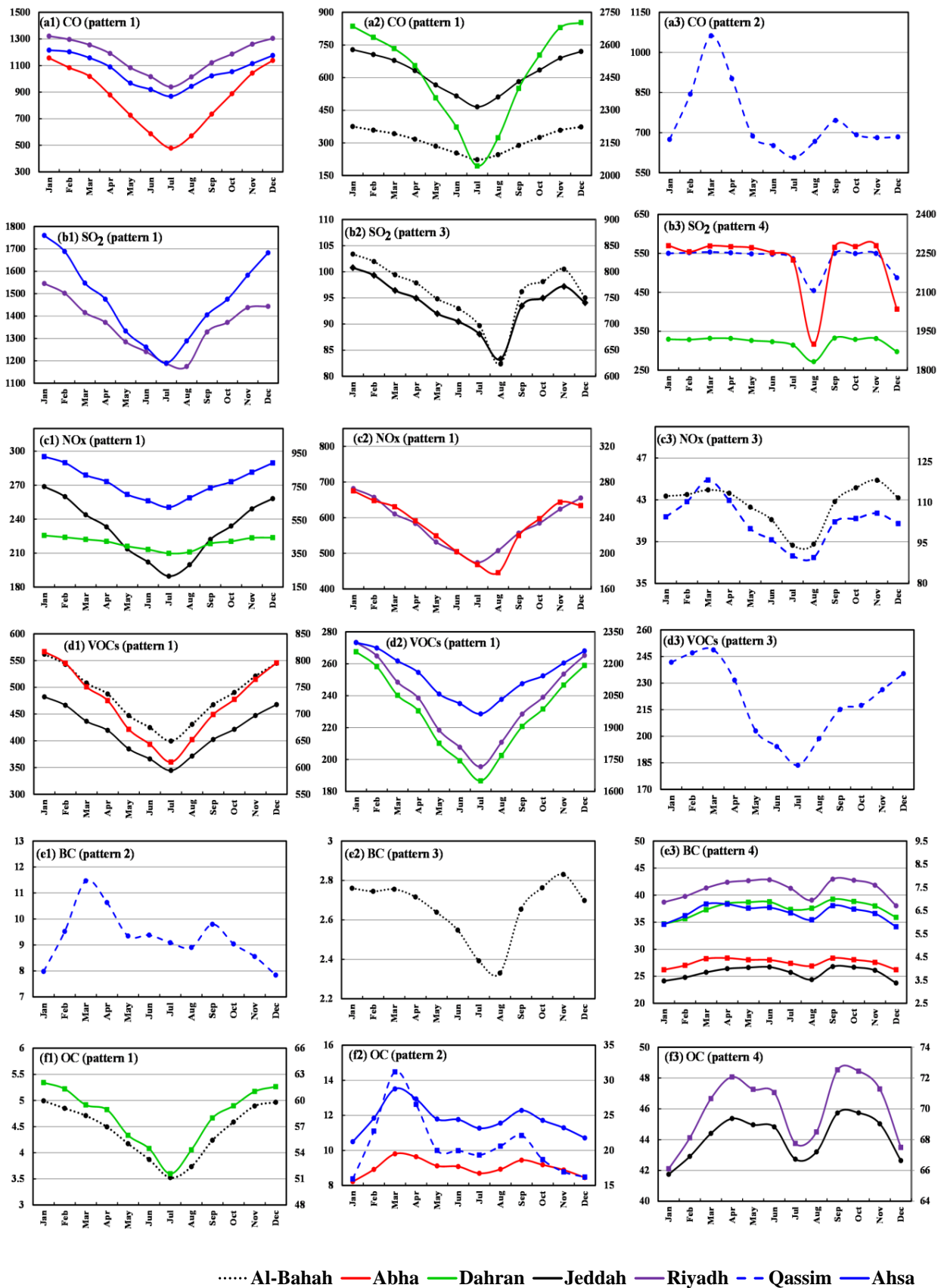


Figure 7. The classified four patterns of the six pollutant emissions based on their annual cycle.



**Figure 8.** The annual cycle of the six pollutant emissions across the period 1960–2020 at the seven KSA stations; the left vertical axis is for curves with circled points, while the right one is for squared points.

Table 4 shows the different patterns followed by each pollutant at the seven KSA stations. CO and VOCs followed pattern 1 at all stations except at Qassim, where they followed Pattern 2 and 3, respectively, while NOx and BC followed pattern 1 and pattern 4, respectively, at all stations except at the Al-Baha and Qassim stations, where they followed pattern 3 and 2, respectively. Additionally, OC followed pattern 1 at the Al-Baha and Dhahran stations and followed pattern 2 at the Abha station and pattern 4 at the rest of the stations, while SO<sub>2</sub> followed pattern 1 at Riyadh and Ahsa, pattern 3 at Al-Baha and Jeddah, and pattern 4 at the other three stations. Additionally, pattern 1 across the seven KSA stations was recorded 21 times followed by 10 times for pattern 4, 7 times for pattern 3, and 4 times for pattern 3. Moreover, pattern 1 and pattern 4 were not detected at the Qassim and Al-Baha stations, respectively, while pattern 2 was detected only at the Abha and Qassim stations and pattern 3 was found at the Al-Baha, Jeddah, Qassim and Ahsa stations.

**Table 4.** The different patterns of the six pollutant emissions at the seven KSA stations.

Pollutant	Jeddah	Al-Baha	Abha	Qassim	Riyadh	Ahsa	Dhahran	Total
P1	CO, NO <sub>x</sub> , VOCs	CO, VOCs, OC	CO, NO <sub>x</sub> , VOCs	—	CO, NO <sub>x</sub> , SO <sub>2</sub> , VOCs	CO, NO <sub>x</sub> , SO <sub>2</sub> , VOCs	CO, NO <sub>x</sub> , VOCs, OC	21
P2	—	—	OC	CO, BC, OC	—	—	—	4
P3	SO <sub>2</sub>	SO <sub>2</sub> , NO <sub>x</sub> , BC	—	NO <sub>x</sub> , VOCs	—	OC	—	7
P4	BC, OC	—	SO <sub>2</sub> , BC	SO <sub>2</sub>	BC, OC	BC	SO <sub>2</sub> , BC	10
Total	6	6	6	6	6	6	6	42

### 4.3. Pollutant Emission Variability

In this section, we will investigate and assess the climate variability, sudden (abrupt) changes, and long-term trends for the selected six pollutants at the seven KSA stations throughout the study period.

#### 4.3.1. Coefficient of Variation (COV)

Figure 9a shows the COV values for the annual emissions of the six pollutants at the seven selected stations in Saudi Arabia, while Figure 9b illustrates the COV values for the seasonal emissions of the six pollutants at the Riyadh station. Only one station (Riyadh) was chosen here for the analysis of COV values for seasonal emissions because its seasonal COV behavior is the same as in the remaining six stations. Generally, the COV values for the annual emissions for each pollutant varies from one station to another. The annual SO<sub>2</sub> and VOCs emissions have the highest and lowest COV, respectively, at all stations. The COV values for annual emissions (Figure 9a) indicate that BC has the highest variability at the Riyadh station, while the other pollutants have the highest variability at the Al-Baha station.

The highest COV values for all pollutants reached about 100% or more, except for VOCs at 55.42%. Additionally, the lowest annual variabilities for CO (37.27%) and NO<sub>x</sub> (42.21%) are at the Abha station, those for SO<sub>2</sub> (71.29%) and OC (27.20%) are at the Dhahran station, for VOCs (19.62%) they are at the Riyadh station, and for BC (6.22%) they are at the Al-Baha station. Moreover, the lowest COV values for the annual emission are detected at Jeddah (31.99%), Riyadh (19.62%), Qassim (35.08%), and Ahsa (32.05%) for VOCs, at Dhahran (27.20%) for OC, at Abha (37.27%) for CO, and at Al-Baha (6.22%) for BC. Furthermore, the COV values for seasonal emissions (Figure 9b) show that both BC and OC pollutants have the highest variability (COV > 100%) followed by SO<sub>2</sub> (COV > 80%) and NO<sub>x</sub> (COV > 50%) during all seasons, while the lowest seasonal variability (COV < 25%) was detected for VOCs followed by CO (COV ≤ 50%) during all seasons.

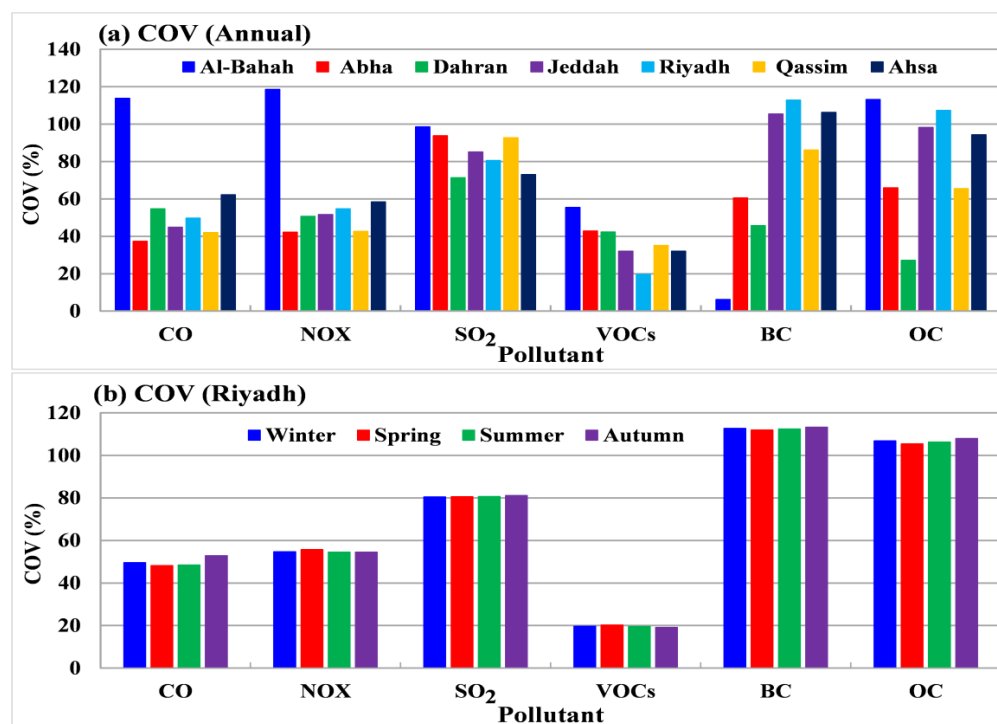


**Figure 9.** The coefficient of variation (COV) for (a) the annual pollutant emissions at 7 KSA stations and (b) the seasonal pollutant emissions at Riyadh station.

#### 4.3.2. Trend Analysis

Figure 10a summarizes the Mann–Kendall (M-K) tau values to investigate the long-term trend for annual pollutant emissions at the seven KSA stations. It was found that CO, NO<sub>x</sub>, SO<sub>2</sub>, and VOCs at all stations along with BC and OC at Al-Baha, Abha, and Dhahran stations have a significant annual positive trend with  $\tau > +0.50$ . The BC has a small annual positive trend ( $\tau < +0.15$ ) at the Qassim station and has a small annual negative trend ( $\tau > -0.15$ ) at the Jeddah, Riyadh, and Ahsa stations. In addition, the OC has a small annual positive trend ( $\tau = +0.2$ ) at the Qassim station and a small annual negative trend ( $\tau > -0.15$ ) at the Ahsa station, while it has a significant annual negative trend ( $\tau < -0.25$ ) at both the Jeddah and Riyadh stations. During all seasons, the emission values of CO, NO<sub>x</sub>, SO<sub>2</sub>, and VOCs have a significant seasonal positive trend ( $\tau > +0.5$ ) at all stations, while OC has a significant seasonal negative trend ( $\tau < -0.25$ ) and BC has a small seasonal negative trend ( $\tau > -0.15$ ). Generally, the annual pollutant emissions have a significant positive trend at all stations except for BC and OC at some stations.

Figure 10b depicts M-K tau values for seasonal emissions for all pollutants at the Riyadh station, in which M-K tau behavior is quite like that of the remaining six stations. It is noticed that the trend for the seasonal pollutant emissions is significantly positive at the Riyadh station except for BC and OC.

The growth rates of emissions are relatively large for SO<sub>2</sub>, NO<sub>x</sub>, and CO because the major sources of these pollutants are energy, industries, and transportation, for which fuel consumption increased significantly along with economic development in the KSA, as found in Section 4.2.2. SO<sub>2</sub>, NO<sub>x</sub>, and CO emissions increased keenly in the early 1990s, along with the rapid growth of the emissions of these pollutants in the KSA. For NO<sub>x</sub>, combustion of oil fuels, especially by transportation, contributed to a large growth in emissions in the latter half of 1960–2020. Growth rates of VOCs have also increased recently due to an increase in the emissions from energy and solvent usage in accordance with the economic growth of the KSA. In addition, the growth rates of BC and OC are relatively small. One reason is that emissions of these pollutants are mainly from incomplete combustion at low temperatures; thus, emissions from energy and industry are relatively small.

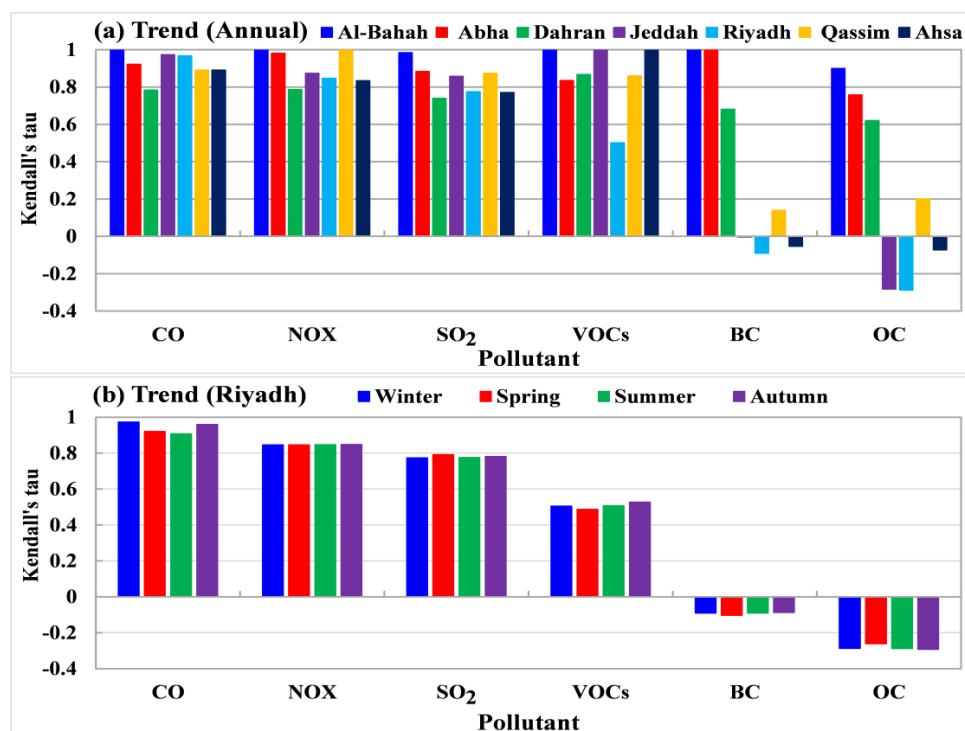


**Figure 10.** Mann–Kendall (M-K) rank statistical test (tau) for (a) the annual pollutant emissions at the selected seven KSA stations and (b) the seasonal pollutant emissions at Riyadh station.

The Kingdom of Saudi Arabia witnessed tremendous development and growth during the period from 1970–2020 because of the oil boom in the early 1970s. The demand for fossil fuels, which is the primary source of energy in the Kingdom, has increased dramatically; for example, it is estimated that fuel consumption in Saudi Arabia increased sixfold in 1981 compared to 1971 [47]. This increase in fuel demand has resulted in a significant increase in SO<sub>2</sub> and NO<sub>x</sub> emissions into the Kingdom's atmosphere. It is shown in [47,48] that desalination plants, which are concentrated on the Red Sea and Arabian Gulf Coasts in the west and east of the KSA, come fourth in the list of fossil fuel consumers in the KSA.

#### 4.3.3. Cumulative Annual Mean

To facilitate the displaying and analysis of the results of the cumulative annual mean (CAM) for the six pollutant emissions, three stations were randomly selected to explain each pollutant as shown in Figure 11. The solid curve line in Figure 11 represents the yearly pollutant emission CAM values, while the dashed straight blue lines show the average value of yearly pollutant emission CAM values along the study period (1960–2020).

It is noted that the CAM values for most pollutant emissions at most stations have a monotonous increase (positive trend) with time during the study period, except for BC, OC, and VOCs at some stations. The CAM values exceeded their reference averages (dashed line in Figure 8) during the 1990s and continued to increase up to the end of the study period, particularly for the pollutants that have a monotonic positive trend. At the Qassim, Riyadh, and Ahsa stations, both BC and OC have a monotonic increase in CAM (positive trend) until 1995, after which their CAM have a monotonic decreasing (negative trend) until the end of the study period. Moreover, VOCs at Riyadh station have a positive CAM trend during the two periods 1960–1972 and 1992–2020, while they have a negative CAM trend during the period from 1972 to 1992. Generally, all pollutants have a positive CAM trend (monotonic increase) at all stations, except for BC and OC after 1992 at some stations, and this in turn explains and agrees with the M-K positive trends (negative for BC and OC) at those stations. Most pollutant emissions, except BC and OC, at most stations exhibited a slight increase during the 1960s and a high increase during the period from 1970 up to the

mid-1990s, followed by a significant increase up to 2020. Meanwhile, BC and OC emissions at most stations (Jeddah, Riyadh, Qassim, and Ahsa) increased gradually from 1960 to the mid-1990s, then decreased gradually up to 2020. In addition, VOC emissions at the Riyadh station increased gradually from 1960 to 1970 and decreased sharply from 1970 to the mid-1990s, then increased gradually up to 2020.

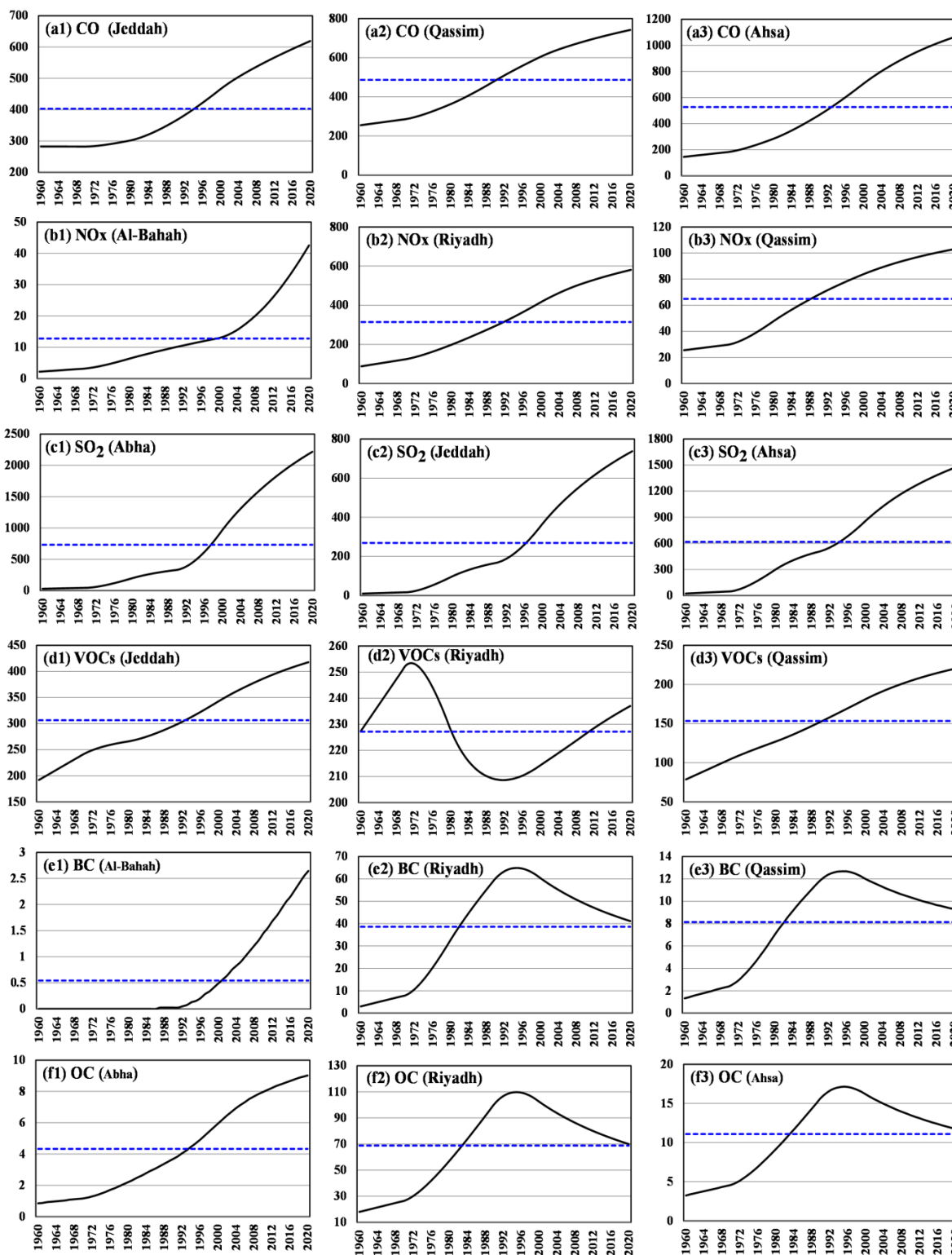


Figure 11. The cumulative annual mean (solid black curve) and its average (blue dashed line) for all pollutant emissions at some stations during the study period (1960–2020); unit:  $\text{kg} \cdot \text{m}^{-2} \times 10^6$ .

#### 4.3.4. Abrupt Change Analysis

The detected abrupt change points within the pollutant emissions timeseries using a Mann–Whitney Z (MWZ) statistics test during the study period (1960–2020) at the seven KSA stations are shown in Figure 12. Figure 12(a1) shows the departure curves of the time series of CO (Jeddah) and illustrates that it has five periods; the first three periods are positive (1960–1969, 1971–1979, and 1981–1989) and the fourth period is negative (2001–2005), while the last period is positive (2006–2020). Figure 12(a2) illustrates that the time series of CO (Qassim) has the same detected abrupt change points as the time series of CO (Jeddah). The Mann–Whitney test detected four positive period abrupt changes in the time series of CO (Ahsa): 1960–1969, 1971–1979, 1981–1989, and 1991–2020, as shown in Figure 12(a3). Figure 12(c1,c2) show the departure curves of the time series of the SO<sub>2</sub> emissions at Abha and Jeddah with the six obvious periods in the study area for the past 61 years: the decrease period is from 2000 to 2005, and the other five periods are the increase periods 1960–1969, 1971–1979, 1981–1989, 1991–1999, and 2006–2020. Moreover, the Whitney test detected five positive period abrupt changes in the time series of VOCs (Jeddah) as illustrated in Figure 12(d1); these periods are 1960–1969, 1971–1979, 1981–1989, 1991–1999, and 2010–2020. The VOCs Whitney test detected five period abrupt changes at Riyadh in the time series as illustrated in Figure 12(d2); the second period is negative (1971–1979) while the other periods are 1960–1969, 1981–1978, 1991–2000, 2001–2010 and 2011–2020. Figure 12(e2,e3) show the departure curves of the time series of the BC emissions at Riyadh and Qassim, which were used to find the five obvious periods in the study area for the past 61 years; the two decrease periods are from 1991 to 2000 and 2001 to 2020, while the other three periods are the increased periods. These periods are 1960–1969, 1971–1979, and 1981–1989.

Figure 13 indicates the frequency of the detected abrupt change years (positive or negative) for the annual pollutant emissions timeseries at the seven KSA stations using the MWZ statistics test. Figure 13 illustrates that there are six detected abrupt change years: 1970, 1980, 1990, 2000, 2005, and 2010. It is obvious that the year 2000 has the highest frequency of abrupt change points (25 positive and 14 negative), while the year 1970 has the second highest frequency of abrupt change points (34 positive and 1 negative). The years 1980 and 1990 have the same frequency of the detected abrupt change points (22), but they vary in frequency in terms of positive or negative abrupt change points, where 1980 has 21 positive and 1 negative abrupt change points while 1990 has 14 positive and 8 negative abrupt change points. The year 2005 has eight positive detected abrupt change points, while the year 2010 has nine positive and one negative abrupt change points.

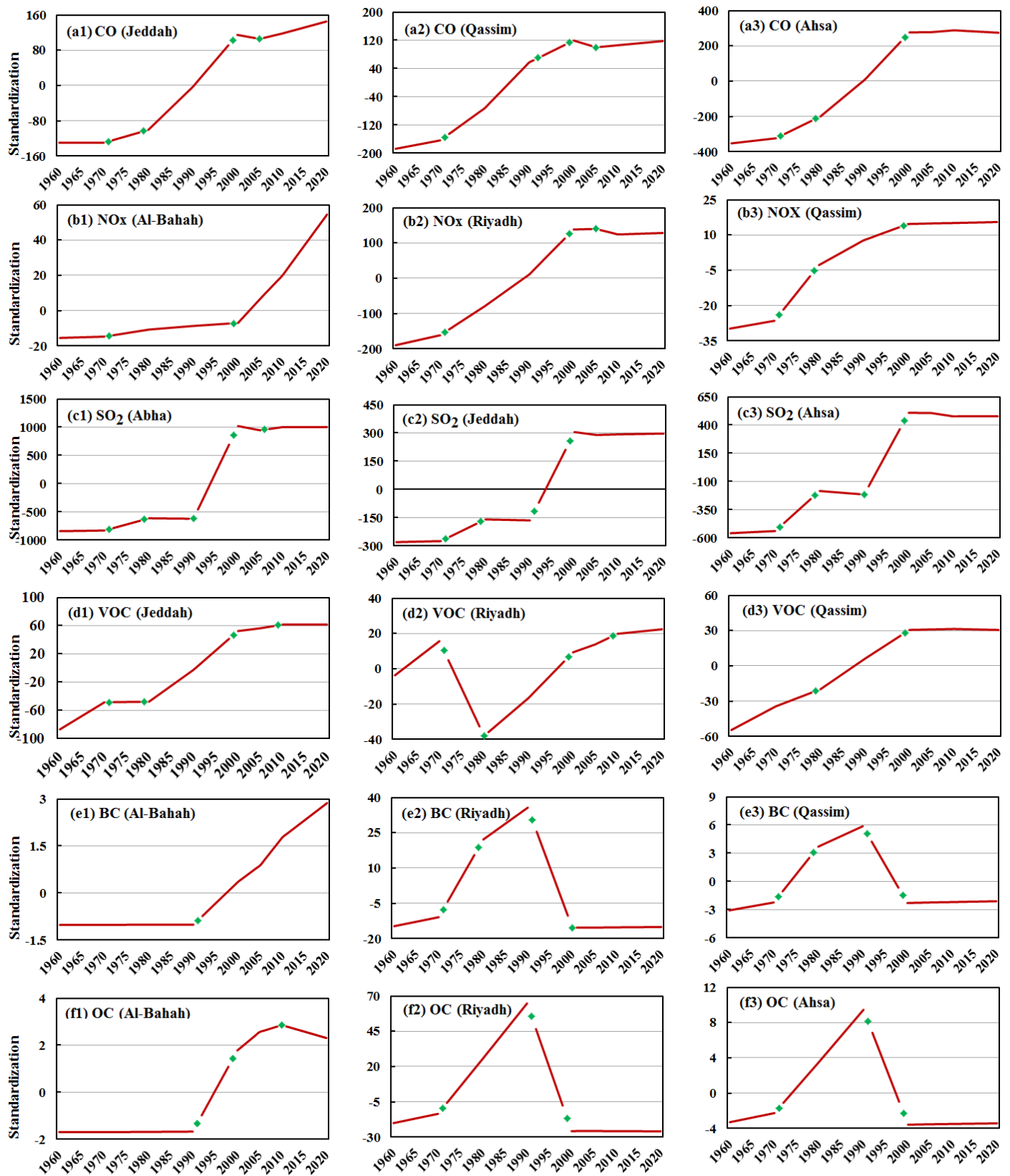
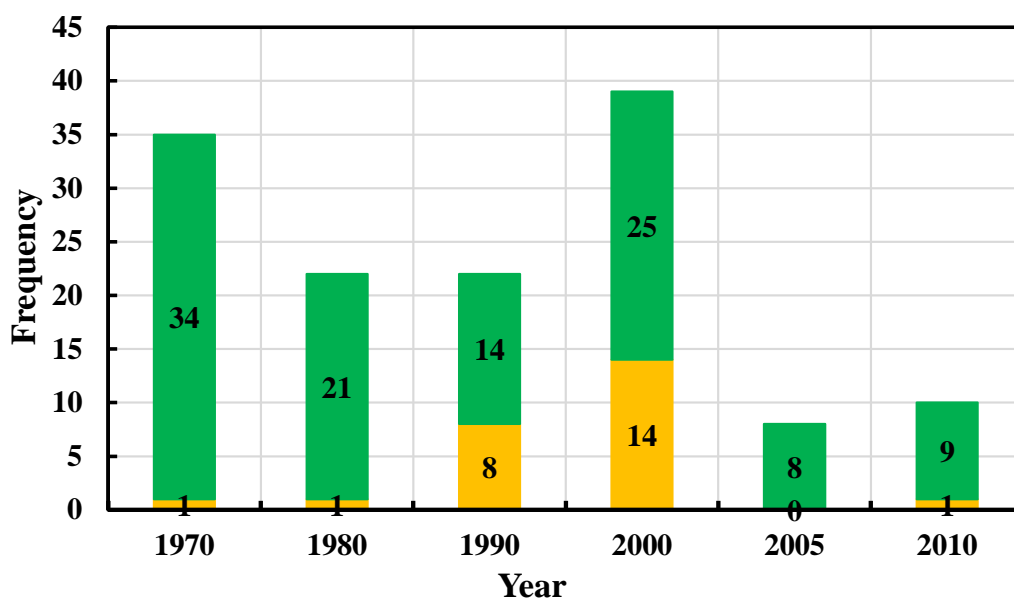


Figure 12. Shifts in the mean for standardization of the annual pollutant emissions during the study period at some KSA stations. Probability = 0.1, cutoff length = 10, Huber parameter = 2.



**Figure 13.** The frequency of the detected years of positive (green) and negative (orange) abrupt changes of the annual pollutant emissions at the seven KSA stations using the MWZ statistics test.

## 5. Conclusions

In this study, the variability, long-term trends, and abrupt changes of six pollutant emissions at seven stations (hotspots) in the Kingdom of Saudi Arabia (KSA) during the period 1960–2020 were studied using monthly MACCity emissions dataset inventories from the different sectors. These pollutants are carbon monoxide (CO), nitrogen oxides (NO<sub>x</sub>), sulfur dioxide (SO<sub>2</sub>), black carbon (BC), organic carbon (OC), and non-methane organic compounds (VOCs). The mapping analysis of annual pollutant emissions revealed that the highest annual emissions (hotspots) can be clearly identified at seven stations (Jeddah, Riyadh Al-Baha, Qassim, Dhahran, Ahsa, and Abha) that cover the western, central, eastern, and southern regions in the KSA.

The climatological monthly mean (annual cycle) of the six pollutant emissions at all stations revealed that there are four distinct patterns for their behaviors across the different months. Pattern 1 contains the emissions that have one interannual wave, while the other three patterns contain the emissions that have two interannual waves. The analysis of different sectors' contributions to the emission of the six pollutants revealed that the energy sector has the highest percentage contribution to the emissions of the six pollutants, with the highest contribution in VOCs (71%). The second one is the transportation sector, which participated at 56% in OC and 54% in BC, while the third one is the industries sector, which has the highest contribution in SO<sub>2</sub> (56%). Furthermore, the coefficient of variation (COV), Mann–Kendall (M-K) rank statistical (tau) test, cumulative annual mean (CAM), and abrupt change detection test were used to achieve the purposes of this study. It is concluded that the COV values for the annual emissions for each pollutant vary from station to other. The annual SO<sub>2</sub> and VOCs emissions have the highest and lowest COV values, respectively, at all stations. BC has the highest variability at the Riyadh station, while the other pollutants have the highest variability at the Al-Baha station. From the M-K rank statistical (tau) test, one can conclude that the annual and seasonal pollutant emissions have significant positive trends at all stations except some small negative trends for BC and OC at some stations. CO, NO<sub>x</sub>, SO<sub>2</sub>, and VOCs at all stations along with BC and OC at the Al-Baha, Abha, and Dhahran stations have a significant annual positive trend, while a significant annual negative trend is recorded for OC at the Jeddah and Riyadh stations. On the other hand, it was found that the CAM values exceeded their climate averages during the 1990s and continued to increase up to 2020, particularly for the pollutants that have a monotonic positive trend. Both BC and OC at the Qassim, Riyadh, and Ahsa stations have

a monotonic increasing in their CAM (positive trend) until 1995 and return to decreasing again (negative trend) up to 2020. Additionally, the VOCs have a positive CAM trend at the Riyadh station during two periods, 1960–1970 and 1990–2020, while they have a negative CAM trend during the period 1970–1990. Overall, the six pollutants have a positive CAM trend (monotonic increase) at all stations, except for BC and OC after 1990 at some stations, and this in turn explains and agrees with the M-K positive trends (negative for BC and OC) at those stations. The analysis of abrupt (sudden) change points showed that the six considered pollutants have six detected abrupt change years: 1970, 1980, 1990, 2000, 2005, and 2010. The development and growth rate in the KSA stated from the early 1970s is attributed to the oil boom. The great increase in pollutant emissions in the early 1980s is due to the increase in fossil fuel demand, which is the primary source of energy in the KSA. Urban development at the beginning of the 1990s led to increasing industries, transportation, and energy consumption, which in turn led to further increase in pollutant emissions up to 2000.

The limitations of this study include the lack of pollutant emissions measurements, which effectively contribute to an accurate understanding and analysis of climatic patterns of pollutant emissions in the KSA. On the other hand, our future work will focus on studying the main factors and causes of pollutant emissions from each sector and their concentration in the different regions of the KSA and their relationship to atmospheric conditions.

**Author Contributions:** Conceptualization, M.A.-M., N.A.-O., A.S., H.A.B. and M.M.; data curation, M.A.-M., N.A.-O., A.S., H.A.B. and M.M.; formal analysis, A.S. and H.A.B.; funding acquisition, M.A.-M.; methodology, A.S., H.A.B. and M.M.; project administration, M.A.-M.; resources, M.A.-M.; software, H.A.B. and M.M.; supervision, M.A.-M., H.A.B. and M.M.; validation, A.S. and H.A.B.; visualization, N.A.-O., A.S., H.A.B. and M.M.; writing—original draft, N.A.-O., A.S., H.A.B. and M.M.; writing—review and editing, M.A.-M., N.A.-O. and H.A.B. All authors have read and agreed to the published version of the manuscript.

**Funding:** This research was funded by the Deputyship for Research & Innovation, Ministry of Education in Saudi Arabia for funding this research work through the project number RI-44-0536.

**Institutional Review Board Statement:** Not applicable.

**Informed Consent Statement:** Not applicable.

**Data Availability Statement:** The data supporting the findings of this article are included within the article and obtained from ECCAD at <https://eccad3.sedoo.fr/metadata/443> (accessed on 1 December 2022).

**Acknowledgments:** The researchers express their great thanks and appreciation to the Deputyship for Research & Innovation, Ministry of Education in Saudi Arabia for funding this research work through the project number RI-44-0536.

**Conflicts of Interest:** The authors declare no conflict of interest.

## References

1. WHO, World Health Organization. *World Report on Ageing and Health*; World Health Organization: Geneva, Switzerland, 2015. Available online: <https://apps.who.int/iris/handle/10665/186463> (accessed on 1 January 2023).
2. WHO. *Ambient Air Pollution: A Global Assessment of Exposure and Burden of Disease*; World Health Organization: Geneva, Switzerland, 2016. Available online: <https://apps.who.int/iris/handle/10665/250141> (accessed on 1 January 2023).
3. Ghude, S.D.; Chate, D.M.; Jena, C.; Beig, G.; Kumar, R.; Barth, M.C.; Pfister, G.G.; Fadnavis, S.; Pithani, P. Premature mortality in India due to PM<sub>2.5</sub> and ozone exposure. *Geophys. Res. Lett.* **2016**, *43*, 4650–4658. [CrossRef]
4. Molina, L.T.; Zhu, T.; Wan, W.; Gurjar, B.R. Impacts of megacities on air quality: Challenges and opportunities. *Oxf. Res. Encycl. Environ. Sci.* **2020**. [CrossRef]
5. Beig, G.; Chate, D.M.; Sahu, S.K.; Parkhi, N.S.; Srinivas, R.; Kausar, A.; Ghude, S.D.; Yadav, S.; Trimbake, H.K. *System of Air Quality Forecasting and Research (SAFAR—India)*; GAW Report No. 217; World Meteorological Organization, Global Atmosphere Watch: Geneva, Switzerland, 2015; p. 51.

6. Ramanathan, V. Climate change, air pollution, and health: Common sources, similar impacts, and common solutions. In *Health of People, Health of Planet and Our Responsibility*; Al-Delaimy, W., Ramanathan, V., Sorondo, M.S., Eds.; Springer Nature: Zurich, Switzerland, 2020; pp. 49–59.
7. Saber, A.; Mohamed, H.; Morsy, M.; El-Hussainy, F.; Eid, M. Characteristics of the simulated pollutants and atmospheric conditions over Egypt. *NRIAG J. Astron. Geophys.* **2020**, *9*, 402–419. [[CrossRef](#)]
8. Saber, A.; Abdallah, A.; Abdel, H.; Mohamed, B.; El-hussainy, F.M. Statistical study of the aerosols emission over Egypt. *Al-Azhar Bull. Sci.* **2017**, *9*, 63–80.
9. Saber, A.; Abdel Basset, H.; Eid, M.M. Historical Study of Pollutants Emission Over Egypt Using ACCMIP Data. *Al-Azhar Bull. Sci.* **2020**, *31*, 1–9. Available online: [https://absb.journals.ekb.eg/article\\_210378.html](https://absb.journals.ekb.eg/article_210378.html) (accessed on 21 March 2022).
10. Singh, P.; Yadav, D. Link between air pollution and global climate change. In *Global Climate Change*, 1st ed.; Singh, S., Singh, P., Rangabhashiyam, S., Srivastava, K.K., Eds.; Elsevier: Amsterdam, The Netherlands, 2021; pp. 79–108.
11. Hemming, W. Transport, Air Pollution and Climate Change: Two Sides of the Same Coin. *Ramphal Inst.* **2021**, *2*, 5. [[CrossRef](#)]
12. Apte, J.S.; Brauer, M.; Cohen, A.J.; Ezzati, M.; Pope III, C.A. Ambient PM<sub>2.5</sub> reduces global and regional life expectancy. *Environ. Sci. Technol. Lett.* **2018**, *5*, 546–551. [[CrossRef](#)]
13. Khodeir, M.; Shamy, M.; Alghamdi, M.; Zhong, M.; Sun, H.; Costa, M.; Chen, L.C.; Maciejczyk, P.M. Source apportionment and elemental composition of PM<sub>2.5</sub> and PM<sub>10</sub> in Jeddah City, Saudi Arabia. *Atmos. Pollut. Res.* **2021**, *3*, 331–340. [[CrossRef](#)]
14. Alam, K.; Trautmann, T.; Blaschke, T.; Subhan, F. Changes in aerosol optical properties due to dust storms in the Middle East and Southwest Asia. *Remote Sens. Environ.* **2014**, *143*, 216–227. [[CrossRef](#)]
15. Farahat, A. Air pollution in the Arabian Peninsula (Saudi Arabia, the United Arab Emirates, Kuwait, Qatar, Bahrain, and Oman): Causes, effects, and aerosol categorization. *Arab. J. Geosci.* **2016**, *9*, 196. [[CrossRef](#)]
16. Farahat, A. Comparative analysis of MODIS, MISR, and AERONET climatology over the Middle East and North Africa. *Ann. Geophys.* **2019**, *37*, 49–64. [[CrossRef](#)]
17. Rahman, S.M.; Khondaker, A.N.; Hasan, M.A.; Reza, I. Greenhouse gas emissions from road transportation in Saudi Arabia—a challenging frontier. *Renew. Sustain. Energy Rev.* **2017**, *69*, 812–821. [[CrossRef](#)]
18. Lim, C.C.; Thurston, G.D.; Shamy, M.; Alghamdi, M.; Khoder, M.; Mohorjy, A.M.; Alkhalaf, A.K.; Brocato, J.; Chen, L.C.; Costa, M. Temporal variations of fine and coarse particulate matter sources in Jeddah, Saudi Arabia. *J. Air Waste Manag. Assoc.* **2018**, *68*, 123–138. [[CrossRef](#)] [[PubMed](#)]
19. Rushdi, A.I.; Al-Mutlaq, K.F.; Al-Otaibi, M.; El-Mubarak, A.H.; Simoneit, B.R. Air quality and elemental enrichment factors of aerosol particulate matter in Riyadh City, Saudi Arabia. *Arab. J. Geosci.* **2013**, *6*, 585–599. [[CrossRef](#)]
20. Alharbi, B.; Shareef, M.M.; Husain, T. Study of chemical characteristics of particulate matter concentrations in Riyadh, Saudi Arabia. *Atmos. Pollut. Res.* **2015**, *6*, 88–98. [[CrossRef](#)]
21. Al-Jeelani, H.A. Air quality assessment at Al-taneem area in the holy Makkah city, Saudi Arabia. *Environ. Monit. Assess.* **2009**, *156*, 211. [[CrossRef](#)]
22. Othman, N.; Jafri, M.Z.M.; San, L.H. Estimating particulate matter concentration over arid region using satellite remote sensing: A case study in Makkah, Saudi Arabia. *Mod. Appl. Sci.* **2010**, *4*, 131. [[CrossRef](#)]
23. Al-Jeelani, H.A. Diurnal and seasonal variations of surface ozone and its precursors in the atmosphere of Yanbu, Saudi Arabia. *J. Environ. Protect.* **2014**, *5*, 408. [[CrossRef](#)]
24. Khalil, M.A.K.; Butenhoff, C.L.; Porter, W.C.; Almazroui, M.; Alkhalaf, A.; Al-Sahafi, M.S. Air quality in Yanbu, Saudi Arabia. *J. Air Waste Manag. Assoc.* **2016**, *66*, 341–355. [[CrossRef](#)]
25. Porter, W.C.; Khalil, M.A.K.; Butenhoff, C.L.; Almazroui, M.; Al-Khalaf, A.K.; Al-Sahafi, M.S. Annual and weekly patterns of ozone and particulate matter in Jeddah, Saudi Arabia. *J. Air Waste Manag. Assoc.* **2014**, *64*, 817–826. [[CrossRef](#)]
26. Rehan, M.; Munir, S. Analysis and Modeling of Air Pollution in Extreme Meteorological Conditions: A Case Study of Jeddah, the Kingdom of Saudi Arabia. *Toxics* **2022**, *10*, 376. [[CrossRef](#)] [[PubMed](#)]
27. Ekholm, T.; Karvosenoja, N.; Tissari, J.; Sokka, L.; Kupiainen, K.; Sippula, O.; Savolahti, M.; Jokiniemi, J.; Savolainen, I. A multi-criteria analysis of climate, health and acidification impacts due to greenhouse gases and air pollution—The case of household-level heating technologies. *Energy Policy* **2014**, *74*, 499–509. [[CrossRef](#)]
28. Rawat, S.S.; Pant, S.; Kumar, A.; Ram, M.; Sharma, H.K.; Kumar, A. A State-of-the-Art Survey on Analytical Hierarchy Process Applications in Sustainable Development. *Int. J. Math. Eng. Manag. Serv.* **2022**, *7*, 883–917. [[CrossRef](#)]
29. Kumar, A.; Garg, P.; Pant, S.; Ram, M.; Kumar, A. Multi-Criteria Decision-Making Techniques for Complex Decision Making Problems. *Math. Eng. Sci. Aerosp. (MESA)* **2022**, *13*, 791–803.
30. Hamad, M.E.; Amer, H.M.; Farrag, M.A.; Osman, A.H.; Almajhdi, F.N. Naked DNA immunization with full-length attachment gene of human respiratory syncytial virus induces safe and protective immune response. *Acta Virol.* **2018**, *62*, 137–146. [[CrossRef](#)]
31. Ibrahim, A.O.; Baqawy, G.A.; Mohamed, M.A.S. Tourism attraction sites: Boasting the booming tourism of Saudi Arabia. *Int. J. Adv. Appl. Sci.* **2021**, *8*, 1–11.
32. Kumar, A.; Abdullah, M.M. An Overview of Origin, Morphology and Distribution of Desert Forms, Sabkhas and Playas of the Rub? Al Khali Desert of the Southern Arabian Peninsula. *Earth Sci. India* **2011**, *4*, 105–135.
33. Stewart, S.A. Structural geology of the Rub’Al-Khali Basin, Saudi Arabia. *Tectonics* **2016**, *35*, 2417–2438. [[CrossRef](#)]
34. Almazroui, M.; Islam, M.N.; Jones, P.D.; Athar, H.; Rahman, M.A. Recent climate change in the Arabian Peninsula: Annual rainfall and temperature analysis of Saudi Arabia for 1978–2009. *Int. J. Clim.* **2012**, *32*, 953–966. [[CrossRef](#)]

35. Chowdhury, S.; Al-Zahrani, M. Implications of climate change on water resources in Saudi Arabia. *Arab. J. Sci. Eng.* **2013**, *38*, 1959–1971. [[CrossRef](#)]
36. Tarawneh, Q.Y.; Chowdhury, S. Trends of climate change in Saudi Arabia: Implications on water resources. *Climate* **2018**, *6*, 8. [[CrossRef](#)]
37. Granier, C.; Bessagnet, B.; Bond, T.; Angiola, A.D.; Van Der Gon, H.D.; Frost, G.J.; Heil, A.; Kaiser, J.W.; Kinne, S.; Klimont, Z.; et al. Evolution of anthropogenic and biomass burning emission of air pollutants at global and regional scales during the 1980–2010 period. *Clim. Chang.* **2011**, *109*, 163–190. [[CrossRef](#)]
38. Lamarque, J.-F.; Shindell, D.T.; Josse, B.; Young, P.J.; Cionni, I.; Eyring, V.; Bergmann, D.; Cameron-Smith, P.; Collins, W.J.; Doherty, R.; et al. The Atmospheric Chemistry and Climate Model Intercomparison Project (ACCMIP): Overview and description of models, simulations and climate diagnostics. *Geosci. Model Dev.* **2013**, *6*, 179–206. [[CrossRef](#)]
39. Mitchell, J.M.; Dzerdzeevskii, B.; Flohn, H.; Hofmery, W.L. *Climatic Change*; WMO Tech. Note 79. WMO No. 195. TP-100; WMO: Geneva, Switzerland, 1966; 79p.
40. Pearson, E.S.; Hartley, H.O. *Biometrika Tables for Statisticians*, 2nd ed.; Cambridge University Press: Cambridge, UK, 1958; Volume 1, 240p.
41. Sneyers, R. *On the Statistical Analysis of Series of Observations*; Technical Note, No. 143; World Meteorological Organization (WMO): Geneva, Switzerland, 1990; 192p.
42. Schonwiese, C.D.; Rapp, J. *Climate Trend Atlas of Europe Based on Observations 1891–1990*; Kluwer Academic Publishers: Dordrecht, The Netherlands, 1997.
43. Hasanean, H.M. Variability of the North Atlantic Subtropical High and Associations with the Tropical Sea Surface Temperature. *Int. J. Climatol.* **2004**, *24*, 945–957. [[CrossRef](#)]
44. Kendall, M.G. *The Measurement of Rank Correlation. Rank Correlation Methods*, 4th ed.; Charles Griffin: London, UK, 1970; pp. 1–18.
45. Al-Kallas, S.; Al-Mutairi, M.; Abdel Basset, H.; Abdeldym, A.; Morsy, M.; Badawy, A. Climatological Study of Ozone over Saudi Arabia. *Atmosphere* **2021**, *12*, 1275. [[CrossRef](#)]
46. Mauget, S. Time series analysis based on running Mann-Whitney Z Statistics. *J. Time Ser. Anal.* **2011**, *32*, 47–53. [[CrossRef](#)]
47. Saudi National Paper on Energy. Energy consumption in the Kingdom of Saudi Arabia 1986 and future projection. In Proceedings of the Arab Fourth Energy Conference, Baghdad, Iraq, March 1988; Volume 4, pp. 1–28.
48. Saudi National Paper on Energy. Energy consumption in the Kingdom of Saudi Arabia in 1983 and future projection. In Proceedings of the Arab Third Energy Conference, Algiers, Algeria, 4–9 May 1985; Volume 7, pp. 159–187.

**Disclaimer/Publisher’s Note:** The statements, opinions and data contained in all publications are solely those of the individual author(s) and contributor(s) and not of MDPI and/or the editor(s). MDPI and/or the editor(s) disclaim responsibility for any injury to people or property resulting from any ideas, methods, instructions or products referred to in the content.